Data Quality of the JERS-1 SAR Global Rain Forest Mapping (GRFM) Project

Bruce Chapman[1], Marcos Alves[1], Masanobu Shimada[2], Tony Freeman[1], Ake Rosenqvist[3] and Paul Siqueira[1]

[1] Jet Propulsion Laboratory, California Institute of Technology

[2] NASDA Earth Observation Research Center

[3] Joint Research Center

Abstract

The National Space Development Agency of Japan's (NASDA) JERS-1 SAR began collecting data in 1995 for the Global Rain Forest Mapping Project (GRFM). The GRFM data quality has been examined for products resulting from both the NASDA and Alaska SAR facility's (ASF) processing facilities. Some radiometric corrections have been applied to the ASF processed data from South and Central America. In general, the calibration of the data from ASF and NASDA is similar, though there are some significant differences. Examples of imagery are presented, along with quantitative analysis of the calibration of the data.

Corresponding author : Bruce Chapman

Jet Propulsion Laboratory M/S 300-227

4800 Oak Grove Dr.

Pasadena, CA 91109

USA

Tel : 1-818-354-3603

Fax : 1-818-393-5285

Email : bruce.chapman@jpl.nasa.gov

1 Introduction

The National Space Development Agency of Japan (NASDA) initiated the Global Rain Forest Mapping Project (GRFM) in 1995 (Rosenqvist, 1996, Freeman *et al*, 1996). The objective of this project is to use the Japanese Earth Remote Sensing satellite (JERS-1) Synthetic Aperture Radar (SAR) to map the world's tropical rain forest regions at high resolution. This joint project between NASDA's Earth Observation Research Center (EORC), NASA's Jet Propulsion Laboratory (JPL), and the Space Applications Institute of the European Commission's Joint Research Center (JRC/SAI) has assembled a team of invited scientists to evaluate, analyze, and use the data.

Data processing for the GRFM project is being done both at NASDA and at the Alaska SAR Facility (ASF) of the University of Alaska at Fairbanks. Imagery from South and Central America will be processed by ASF, while imagery from Africa, S.E. Asia, and Australia will be processed by NASDA.

The processing facilities were developed independently; therefore, there are some differences in the final image products. This paper will describe and quantify the similarities and differences, while characterizing the resulting image products.

1.1 *Description of JERS-1*

The JERS-1 satellite (also known as Fuyo-1) was launched on February 11, 1992 by a two stage HI rocket from the Tanegashima Space Center into a sun-synchronous polar orbit (inclination 97.67 deg). The spacecraft has an altitude 568 km over the equator, and exactly repeats 659 revolutions every 44 days. The satellite carries two instruments - a SAR and an optical sensor (OPS) - and a data recorder (MDR). The MDR can record up to 8 minutes of data (corresponding to a data take about 75km wide by 3,000 km long) outside the ground station coverages, and downlink the data to either ASF or NASDA's

Earth Observation Center (EOC). In 1994, the JERS-1 satellite completed its 2 year mission, and since then has been operating in an extended mission by NASDA. Only the SAR sensor and data will be discussed here.(NASDA EOC, 1995)

1.2 *SAR sensor description*

Table 1 summarizes the basic characteristics of the JERS-1 SAR.

A few months after launch, a malfunction within the SAR instrumentation (arcing between two of the SAR antenna sub-panels) resulted in the SAR operating at half of its designed power output, generating lower than planned signal to noise ratios and a higher than planned noise equivalent σ^0 (normalized radar backscatter coefficient). In addition, due to concerns about an on-board battery, the JERS-1 SAR can usually only acquire data during a descending (southerly) path of the orbit (due to an unrelated electrical problem).

1.3 *Data processing*

Processing facilities for JERS-1 SAR data exist at both NASDA and ASF. Each processing center can process JERS-1 data to calibrated full resolution of 12.5 meter pixel spacing in both range and azimuth. Each processing facility incorporates the CEOS format for the data products, but the header records and the data format are different (see section 2).

At the time of the initiation of the GRFM project, both the NASDA and ASF processors consisted of specially designed hardware processors and associated software driven computer interfaces between the SAR correlator and other components. The NASDA processor, developed by NEC under a NASDA contract, is operated under contract to NASDA by the Remote Sensing Technology Center of Japan (RESTEC). The ASF processor was developed by JPL, and is operated by ASF for NASA. As of 1997, the ASF processor can process data from NASDA's JERS-1 SAR, from the

European Space Agency's (ESA) Earth Remote Sensing Satellite (ERS-1 and ERS-2) SAR, and from the Canadian Space Agency's (CSA) Radarsat SAR.

Prior to 1996, the NASDA processor produced an artifact in all of its image products that manifested itself as "bands" in both range and azimuth directions (though the banding was most evident in the azimuth direction). These bands were due to residual calibration errors of the Sensitivity Time Control (STC) signal attenuation. The magnitude and location of these bands varied slightly from scene to scene. Usually, the magnitude of the banding was less than 0.5 dB, and four or five bands were evident across the image. In addition, sometimes a linear radiometric trend of less than 1 dB in the range direction was present. In mid-1996, prior to processing GRFM data, this error in the processor was corrected. See figure 1 for an example of the imagery prior to correction of the processing artifact.

The NASDA processor can process about 45 scenes per 16 hour day, while the ASF processor can process about 100 JERS-1 scenes per 16 hour day (though in both cases, non-GRFM data processing is performed. In the case of ASF, only a small fraction of the processing throughput is used for the GRFM project).

1.4 *Description of GRFM*

The GRFM project to map the world's rain forest regions will not be completed until 1999 due to the large amounts of data to be processed. Approximately 40 million square kilometers consisting of 5 TeraBytes of imagery will be generated. This imagery will be distributed over the internet and on CD-ROM to scientists studying the regions imaged.

For the imagery from South and Central America, ASF will process and calibrate the data to full resolution. JPL will verify the calibration of the data, and generate low

resolution data products (100 m pixel spacing) of the radar backscatter and the image texture. Both NASDA and JPL are producing mosaics of the data to span the entire continent from these low resolution image products. A team from the University of California - Santa Barbara (UCSB), working with their colleagues from the Brazilian National Institute for Space Research (INPE) and from the National Institute for Research of the Amazon (INPA), have collected ground validation data from regions near the Amazon River to verify the geometric accuracy of the data.

For the imagery from Western and Central Africa, NASDA will process and calibrate the data to full resolution. JRC/SAI will generate a variety of lower resolution data products and mosaics, and compare the results with ERS-1 data.

For the imagery from S. E. Asia and Australia, NASDA will process and calibrate the data to full resolution, and generate low resolution data products and mosaics.

Many of the GRFM principle investigators will analyze data from these datasets to fulfill their individual scientific objectives. More information about the GRFM project may be found at the following web site : http://southport.jpl.nasa.gov/GRFM/ .

1.5 *Data products*

The GRFM project anticipates several different kinds of data products being generated. See table 2 for a summary description of several proposed data products. These different data products are being generated by several different data processing centers - NASDA, ASF, JPL, and JRC.

For each of these data products, the image file may be stored in a variety of data formats. For example, the JPL low resolution data is stored in the ASF CEOS format and as a GIF image (since GIF compression is loss-free, σ^0 may be accurately retrieved from the GIF images as well).

1.6 *Coverage*

The JERS-1 SAR acquired GRFM data between September 1995 and February 1997. Since the L-band (1275 MHz) wavelength of the radar is sensitive to flooded forest conditions, some areas were mapped twice so that the extent of inundation that occurs along major river systems such as the Amazon or Congo rivers can be estimated. Figure 2a shows the coverage obtained for South America between September 27 and December 12, 1995. Figure 2b shows the coverage obtained between May 4 and August 13, 1996 for Central and South America. Figures 3a and 3b shows the coverage of Western and Central Africa, and figure 4 the coverage of S.E. Asia, and Australia.

1.7 *Data access*

GRFM data products will be made available to the science community by CD-ROM and by the world wide web. Currently, at a web site at JPL (http://southport.jpl.nasa.gov/GRFM/), available data products can be downloaded for scientific research and analysis. Similar web sites exist at the NASDA and JRC/SAI home pages, as well as other sites, and are linked together. CD-ROM's from the GRFM project have been available since March 1998, and may be obtained by writing the authors.

1.8 *Calibration data*

In addition to the GRFM data, the JERS-1 SAR has acquired data from almost every land surface region on Earth. In order to validate the calibration of the data, some non-GRFM data has been analyzed. In particular, corner reflectors have been placed in Japan (Niigata and Hatoyama), the USA (Edward's calibration array in Southern California), Alaska (Delta Junction), and Brazil (Manaus) and their backscatter analyzed (see section 3). The corner reflectors were oriented for maximum radar backscatter for the JERS-1 SAR.

To assess the relative radiometric calibration for range and azimuth dependent calibration errors, such as may be introduced by inaccurate knowledge of the antenna pattern, large uniform rain forest regions within South America were analyzed. The relative calibration of both NASDA and ASF processed data were verified in this way.

The corner reflector arrays in Japan are monitored periodically to verify the NASDA calibration constant and SAR system performance.

2 Comparison between NASDA and ASF Processing

The NASDA and ASF processing facilities both generate full resolution imagery with a pixel spacing of 12.5 m in both the range and azimuth (along track and cross track) directions. The NASDA 2.1 level data product is projected to UTM coordinates , while the ASF projection for data is a constant ground pixel spacing in both range and azimuth. Both processing facilities produce CEOS formatted data.

The calibration factor to convert the digital number (d_n) values to σ^0 differs between NASDA and ASF processed imagery. For ASF processed imagery, the calibration factor (linear) may be found in the CEOS leader file. For NASDA processed imagery, see Table 4. NASDA carefully monitors backscatter from corner reflectors and updates the calibration factor when analysis of the data so indicates. The dates given below correspond to the date of acquisition of the data.

In order to calculate the normalized radar backscatter (σ^0) from NASDA or ASF processed imagery (ignoring noise) :

$$\sigma^0 = 20\log_{10}(d_n) + F \qquad (1)$$

where σ^0 is the normalized radar backscatter in dB, d_n is the digital number, and F is the calibration factor in dB. This formula works for all products derived from the NASDA or ASF imagery, including mosaic products and low resolution imagery. If the noise vector is known, it is possible to remove the noise floor by the following formula :

$$\sigma^0 = 10\log_{10}\{f\,(d_n)^2 - f_n N(r)\} \qquad (2)$$

where σ^0 is the normalized radar backscatter in dB, d_n is the digital number, f is the linear value of the calibration factor, f_n is the noise conversion factor, and N(r) is the normalized noise value as a function of range. For ASF processed imagery, N(r) may be found in the CEOS leader file and ranges between 0 and 1, while f_n may be calculated from two calibration constants found in the CEOS leader file (the linear absolute calibration factor and the noise scale factor) by finding the product of the two. Typically :

$$f_n = 4.547\text{x}10^{-2} \text{ (typically)} \qquad (3)$$

For the NASDA data products, each scene of data corresponds geographically to the JERS-1 Row/Path definition (NASDA EOC, 1995). There are three CEOS files associated with each scene : a leader file, an image file, and a trailer file. The leader and trailer files are ASCII header files, while the image file is a binary data file. A detailed description of these files may be found in (NASDA EOC, 1996). Each line of data in the image file is preceded by 12 bytes of prefix information.

For the ASF data products, each scene is identified by the rev number since launch, and the center latitude. Each frame of data has two associated CEOS files : a leader file and an image file. The header information in the ASCII leader file is organized quite differently

from that produced by NASDA, but much of the same information is present, with the notable exception that the ASF leader file includes an estimate of the range dependent noise equivalent σ^0. The format of the ASF files changed in 1996. Prior to late 1996, the image files were preceded on each line with a 12 byte prefix and there was also an ASCII CEOS trailer file. After late 1996, the prefix length increased to 192 bytes. There were changes to the header information as well. (Bicknell, 1997)

The most significant difference between the NASDA and ASF data products is that the NASDA image product stores the d_n values as 16 bit values while the ASF image product is 8 bit. However, a d_n value of 4096 (from the NASDA image products) (which requires 12 bits) corresponds to a σ^0 of +3.7 dB (assuming a calibration constant of -68.5 dB), a backscatter value which is generally larger than is normally seen in an image with natural targets. Therefore, for most scenes of natural targets, less than 12 of the 16 bits are being used by the NASDA image product. In addition, the d_n value of the noise floor (corresponding to σ^0 as low as -20 dB) is about 265; it is therefore rare to find a d_n value less than 265.

If the calibration constant for an ASF image product is standard (i.e. -48.54 dB), then a d_n of 255 corresponds to a σ^0 of only -0.4 dB. This is a low value to saturate at, as some flooded forests will have σ^0 values larger than that.

At low backscatter values (σ^0 = -14 dB), which roughly corresponds to imagery of open water and low vegetation areas, each change in d_n for ASF imagery indicates a change of 0.17 dB in σ^0, a rather large quantization. For NASDA imagery, at σ^0 =-14 dB, each change in d_n indicates a change of only 0.02 dB. The d_n value of the noise floor (corresponding to σ^0 as low as -20 dB) for ASF image products is about 26, where each change in d_n corresponds to a change in σ^0 of 0.34 dB (but only 0.03 for NASDA image products).

Figure 5 shows a histogram of the values found in a typical NASDA and ASF image over a rain forest region.

3 Radiometric Calibration

Verification and correction of radiometric calibration errors in the ASF processed imagery was performed prior to mosaicking the data (Siqueira *et al*, 1998). After the data was mosaicked, it was then possible to assess more accurately and completely the quality of the calibration verification process.

3.1 *Absolute calibration*

The absolute calibration of the JERS-1 SAR data was verified by analysis of corner reflectors in Southern California, USA; Delta Junction, Alaska; and Manaus, Brazil (vanZyl *et al*, 1992). Tables 5 and 6 list the result for several corner reflectors imaged in 1992 and 1993 by the JERS-1 SAR and processed by the NASDA and ASF processors. The results indicate that the calibration factors from table 4 are accurate to better than 1 dB.

In order to assess the correspondence in absolute calibration between ASF and NASDA processed imagery, a JERS-1 datatake of a region of uniform rain forest in South America was processed by the both ASF and NASDA processing facilities, and the results analyzed. Since the same raw signal data was processed, the difference between the two image products is due solely to processing differences (including standard calibration) between the ASF and NASDA processors. Analysis showed that there was a slight difference in absolute calibration between the two facilities, whereby the ASF processor calibration is 0.8 dB brighter than that of NASDA. This error is less than that of the accuracy of the absolute calibration.

3.2 *Relative Calibration*

The relative calibration between scenes and within each scene must be excellent if a seamless image mosaic product is desired. Errors in σ^0 greater than about 0.2 dB will negatively impact the appearance and analysis of the GRFM mosaic image products. As the data is averaged down, banding in the data becomes even more noticeable. Therefore, for the data acquired of South and Central America, JPL performed a careful verification of the relative calibration of the JERS-1 SAR imagery as processed by ASF.

During processing at both ASF and NASDA, a standard correction is applied to account for the change in antenna gain with look angle. During ASF processing, the inverse of this gain factor is saved as the "noise vector" in the CEOS leader file, and a typical example is shown in figure 6. This antenna gain is accurately measured and analyzed both before and after launch, but it is not unusual for there to be discrepancies between the actual antenna pattern and the applied antenna pattern on the order of 0.5 dB.

Since even this small level of error can introduce significant problems when mosaicking the data, the following procedure was used to verify the relative calibration of JERS-1 data over the Amazon from the ASF imagery, and correct it if necessary :

First, each ASF full resolution image was averaged to 100 m pixel spacing in both the range and azimuth directions (8x8 pixels). The description of the analysis that follows was derived from the low resolution imagery, but the results may be applied to either the low or full resolution imagery.

A large sample of ASF imagery was analyzed to determine whether any correction to the radiometric calibration was necessary. A geographically and temporally diverse sample of images was selected, where uniform, undisturbed forest areas were binned and averaged in the cross track (range) direction. Uniform rain forests are relatively easy to identify on the SAR imagery - the key areas to avoid are low vegetation and open water

regions. The radar backscatter varies by about 0.6 dB between the near, mid, and far range of the image swath. After averaging a few dozen images containing only uniform rain forest regions, a consistent curve shape (both magnitude and location) was observed. See figure 7 for a polynomial fit as a function of range. The incidence angle over this range varies between 34 and 43 degrees, over the course of which the scattering from the surface will change slightly, but this effect alone is unlikely to account for the magnitude of the curvature of the radar backscatter.

If there were no radiometric corrections necessary, then we would expect the radar backscatter versus range for uniform rain forest regions to be relatively constant. The polynomial fit shown in figure 8 was divided into each image in order to attempt to correct for an apparent error in all of the imagery, and assumes that the error that was observed in the selected subset would apply to all the imagery. Some images were then examined to insure that the radar backscatter of uniform forest areas as a function of range was indeed constant (see figure 8 for a typical example of the residual errors after correction). In order to maintain the same absolute calibration, the polynomial was normalized such that the average gain was unity.

Out of 1723 scenes between September 27 and December 12, 1992, same radiometric correction as a function of range was applied for 1666 scenes, or 97%. The remaining scenes required a unique radiometric correction. Usually, several adjacent scenes within the same data take required the same unique radiometric correction. Again, using uniform rain forest regions to estimate the trend in the error, a polynomial fit to the data was determined and applied against the image swaths.

3.3 *Noise Equivalent* σ^0

The noise equivalent σ^0 changes as a function of range due to the change in gain of the antenna as a function of look angle. See figure 9 for a typical plot of the noise equivalent σ^0, estimated by analyzing the radar backscatter over open water (generally the darkest locations in the imagery) at several cross-track (range) locations. These areas are generally dominated by noise, rather than signal from the waves on the water.

These plots indicate that at worst the noise equivalent σ^0 is -15 dB, though these values occur over a small range in incidence angles (near and far swath), while at the middle of the swath, the noise equivalent σ^0 is about -20 dB. However, after mosaicking, knowledge of the incidence angle is lost; due to the 30% overlap between scenes, the noise equivalent σ^0 is usually better than -18 dB in the mosaicked images.

3.4 *Calibration errors*

There are two types of remaining calibration errors, one of which can be easily corrected. A calibration log has been kept to determine the calibration procedures that were applied to each scene.

1) absolute calibration error

Occasionally (41 out of 1723 ASF scenes from South America), the absolute calibration of an image appears to be incorrect. This may be determined during mosaicking, and also from examination of a plot of the radiometry versus range for a scene. The cause for this error is unknown, but it is easily corrected if there are targets or regions within the scene of known radar backscatter, such as rain forest regions, whose backscatter is relatively well known. Also, if this scene has scenes that overlap with it (which is generally the case with the GRFM data), then the overlapping regions may be

exactly compared, and the errant image corrected. Most images will be corrected, but there may still remain errors on the order of less than 1 dB that are not corrected.

2) residual range dependent calibration error

Based on the assumption that any calibration error across track is due to an error in the antenna pattern, then we would expect that all scenes would require the same correction. Therefore, if at all feasible, the same radiometric correction was applied to each scene. However, some scenes, after careful scrutiny, required a unique radiometric correction. This correction was recorded so that the process would be reversible for other investigators using the data.

Even after the above corrections were made, the mosaicked images still sometime showed some calibration offsets from surrounding images. Usually the magnitude of this difference is relatively small (0.2 to 0.6 dB). However, in these cases, no attempt was made to correct these images.

The effect of the residual calibration errors is most pronounced when looking at mosaics of images. However, the data quality of the mosaics is no worse than that of the individual scenes, except that the range to each target is no longer known. For instance, it is no longer possible to compare the noise equivalent σ^0 with the range of a target in a scene.

4 Image Quality

In order to assess the resolution in both the azimuth and range direction, and to estimate the Peak Side Lobe Ratio (PSLR), corner reflectors analysis was performed. For NASDA processed imagery, 8 corner reflectors were analyzed, while for ASF imagery, 6 corner reflectors were analyzed. These were the same corner reflectors used to verify the absolute calibration of the data.

As can be seen from table 7, the azimuth resolution of the ASF processed imagery is about 32 m, as opposed to 18 m for NASDA processed imagery. While ASF performs 4 look processing, the NASDA processor processes fewer looks (3) in order to obtain higher resolution.

The estimated PSLR of the data is different between the ASF and NASDA processors, with the PSLR lower for NASDA processed imagery by 5-6 dB.

5 Geometric Accuracy

In order to assess the geometric accuracy of the data, results from the mosaicking of the ASF processed data were utilized. First, mosaicking 1500 adjacent ASF scenes from South America resulted in histograms of offsets in the x and y directions (figure 10). The average offset in x (Longitude) was 317± 2136 meters, while the average offset in y (Latitude) was -1053± 1250 meters. These offsets with respect to the corner latitude/longitudes (retrieved from the CEOS header) roughly indicate the accuracy of knowledge in absolute location, as determined from the satellite ephemeris by the ASF processor.

The mosaicked imagery has been projected into the equiangular projection, in which each pixel is fixed number of arc seconds of latitude and longitude, and where the latitude and longitude meet at right angles.

A more detailed description of the geometric accuracy of the mosaicked GRFM data is deferred to another publication (Siqueira *et al*, 1998).

6 Imagery examples

As the processing is completed, the mosaics of JERS-1 images will be released via CD-ROM. Copies of these CD-ROMs may be obtained by contacting the authors, or by checking the web site for ordering information (http://southport.jpl.nasa.gov/GRFM/).

Figure 11 shows an image of the Balbinas Reservoir in Amazonas (from images averaged to 100 meter pixel spacing), Brazil, several hundred kilometers North of the city of Manaus. General characteristics of this image are as follows:

1) Rivers and areas of open water usually appear very dark, usually approaching the noise floor of the data. In fact, at near and far range, open water is often dominated by noise. Occasionally, if the water is roughened by wind or rain, the signal may increase.

2) Flooded forest areas are bright. This is due to "double bounce" scattering between the trunks of the trees and the underlying water.

3) Areas of low vegetation are in some cases as dark as open water, but in other cases slightly brighter. Factors affecting the radar brightness of these areas include soil moisture and the presence of agriculture.

4) The brightness of the undisturbed forests is less than that of flooded forests, but greater than that of low vegetation.

Figure 12 shows an example of mosaicking two cross track scenes covering the area where the Tapajos and Amazon Rivers converge. As can be seen, the signal from the open water of the Tapajos River is larger in the Westernmost image. This is due to an increase in noise at the near range of the Western image, as compared to the signal at the far range of the Eastern image.

Figure 13 shows an image mosaic of two images where residual calibration errors are evident. A comparison of σ° values within the overlap regions shows a difference of 0.6 dB. See figure 14 for a "slice" through the mismatched images. Fourteen kilometers South from this slice through the data, where the residual calibration error is no longer as evident, the difference in σ° is less than 0.1 dB.

7 Science Content

The tropical rainforests imaged by the GRFM project are of keen interest to both the public and the scientific community. SAR imagery has advantages and disadvantages with respect to optical remote sensing techniques for studying these areas, but unquestionably this data set will be quite useful for characterizing the state of the world's rainforest during the 1995-1997 time frame.

The JERS-1 SAR, and L-band imagery in general, have been shown to be sensitive to flooding conditions, and in particular, flooded forests. (Hess *et al*, 1995) The impact of flooding on the rate of carbon exchange makes inundation extent an important parameter in global climate and climate change models. In addition, inundation areas harbor different plant and animal species than the surrounding rainforest, as well as affecting the nature of human habitation and development. The GRFM project has targeted this utility to map inundation by attempting as much as possible to image areas at both high and low flood seasons.

JERS-1 SAR data is also sensitive, within certain ranges, to variations in biomass (Luckman *et al*, 1997). Therefore, though constrained by a low signal to noise ratio, it is possible using JERS-1 data to differentiate between some vegetation structures, such as cleared fields from mature rainforests. The extent at which the JERS-1 SAR data can be used to differentiate vegetation classes is a topic of current research.

There are other applications being investigated that employ derived products (i.e. measurements of the standard deviation of the imagery) and imagery from other instruments to infer scientific results. The use of JERS-1 SAR to "fill in" missing coverage and to increase the likelihood of success in the classification of forest types by combination of the data with optical and other radar remote sensing data is currently being investigated.

8 Conclusions

The GRFM data quality has been examined for products resulting from both the NASDA and ASF processing facilities. Some radiometric corrections have been applied to the ASF processed data from South and Central America. In general, the calibration of the data from ASF and NASDA is similar, though there are some significant differences. More information can be found at the GRFM web site at JPL (http://southport.jpl.nasa.gov/GRFM/). Some calibration errors still persist in the data, which in further work we hope to correct.

Acknowledgments

The authors wish to thank Japan's National Space Development Agency's Earth Observation Research Center for establishing the Global Rain forest Mapping Project and the Alaska SAR Facility for processing the data from South and Central America. We would also like to thank Erika Podest, Laura Hess, and Greg McGarragh. The work described in this publication was partially carried out by the Jet Propulsion Laboratory, California Institute of Technology, under a contract with the National Aeronautics and Space Administration.

References

CHAPMAN, B., HOLT, J.W., AND HESS, L., 1997, Mapping the extent of inundation of the Amazon River basin, *AGU Fall meeting.,H32A-34, San Francisco, California, 1997.*

FREEMAN, A, CHAPMAN, B., AND ALVES, M.,1996, The JERS-1 Amazon Multi-mission Mapping Study (JAMMS), *Proc of 1996 Intnl. Geosci. Rem. Sens., pp830-833, Lincoln, Nebraska, 1996.*

JET PROPULSION LABORATORY, 1991, Alaska SAR facility Archive and Catalog Subsystem User's Guide, JPL D-5496, Jet Propulsion Laboratory, Pasadena, California, USA.

NASDA EARTH OBSERVATION CENTER, 1995, JERS-1 SAR Data Users Handbook, NASDA EORC, Tokyo, Japan.

NASDA EARTH OBSERVATION CENTER, 1996, JERS SAR/ ERS AMI Image Data Format, First Issue, NASDA EORC, Tokyo, Japan.

ROSENQVIST, AKE , 1996, The global rain forest mapping project by JERS-1 SAR , Proc of XVIII ISPRS Cong. In Vienna, Austria, 1996.

SIQUIERA, P., HENSLEY, S., SHAFFER, S., HESS, L., MCGARRAGH, G., CHAPMAN, B., HOLT, J., AND FREEMAN, A., 1998,A continental scale mosaic of the amazon basin using JERS-1 SAR, submitted to *IEEE Transactions Geoscience and Remote Sensing.*

VANZYL, J., CHAPMAN, B., DUBOIS, PASCALE C., AND FREEMAN, A., 1992, POLCAL User's Manual version 4.0, JPL Internal Document, D-7715, Jet Propulsion Laboratory, California Institute of Technology, Pasadena, California, USA.

YONEYAMA, K., KOIZUMI, T., SUZUKI, T., KURAMASU, T., ARAKI, T., ISHIDA, C., KOBAYASHI, M., AND KAKUICHI, O., 1989, JERS-1 Development Status, *4th Congress of the International Astronautical Federation, Malaga, Spain, October 1989.*

Tables

	JERS-1
Frequency band	L (1275 MHz)
Polarization	HH
Bandwidth	15 Mhz
PRF	1505-1606 Hz
Antenna size	11.9mx2.4 m
Transmitted power	325 W
Repeat orbit	44 days
Incidence angle	38.5 degrees
Look direction	right looking

Table 1. JERS-1 characteristics

Data product	Pixel spacing	Dimension
NASDA Hi-res	12.5mx12.5m	75kmx80km
NASDA low-res	100mx100m	75x80km
ASF Hi-res	12.5mx12.5m	75kmx102.4km
JPL/ASF low res	100mx100m	75kmx102.4km
JPL/ASF texture	100mx100m	75kmx102.4km
JRC/NASDA texture	100mx100m	75kmx80km
JRC/NASDA standard mosaics	100mx100m	5degx5deg
JRC/NASDA low res mosaics	TBD	5degx5deg
NASDA standard mosaics	3"x3"	5degx5deg
JPL/ASF standard mosaics	3 "x3"	5degx5deg
JPL/ASF hi-res mosaics	TBD	TBD
JPL/ASF low-res mosaics	15"x15"	5 degx5deg

Table 2 : planned data products

	ASF	NASDA
data format	8 bit	16 bit
range resolution	18m	18m
azimuth resolution	32m	18m
no. Looks	4	3
header	CEOS	CEOS
image size (pixels)	8192x8192	6100x6400
pixel spacing	12.5 m x 12.5 m	12.5 m x 12.5 m
image size (ground)	75kmx102.4km	75kmx80km
projection	ground (sch)	ground (UTM)
image designation	rev/lat	row/path
noise vector in header	yes	no

Table 3 : comparison of ASF and NASDA image products

	NASDA calibration factor F (db)	linear value f
Feb 1992 - Feb 14, 1993	-70.0	1.000×10^{-7}
Feb 15, 1993 - Oct 31, 1996	-68.5	1.413×10^{-7}
November 1, 1996 -	-68.3	1.479×10^{-7}
	ASF calibration factor F (db)	**linear value f.**
typical value **(found in ceos leader file)**	-48.54	1.400×10^{-5}

Table 4 : calibration factors

Scene	Image ID	Overflight Date	calibration offset (dB)
Edwards	c0077a10	93 Apr 30	-0.61
Edwards	c0077a10	93 Apr 30	-0.85
Edwards	c0077a10	93 Apr 30	-0.78
Edwards	c0077a10	93 Apr 30	-0.80
Edwards	c0077a10	93 Apr 30	0.28
Manaus	c0230b19	93 Jul 06	0.31

Table 5 : NASDA processed imagery - corner reflector analysis

Scene	Image ID	rev	Overflight Date	calibration offset (dB)
Delta Junction	1000346	2528	92 Jul 28	0.13
Delta Junction	1000348	3816	92 Oct 22	-0.56
Delta Junction	1000350	3831	92 Oct 23	-1.4
Delta Junction	1000353	3861	92 Oct 25	0.70
Delta Junction	1000355	3876	92 Oct 26	0.92

Table 6 : ASF processed imagery - corner reflector analysis

	Range Res. (m)	Azimuth Res. (m)	Range PSLR (dB)	Azimuth PSLR (dB)
NASDA	18.2 ± 0.6	18.2 ± 1.8	-13.7 ± 2.0	-21.1 ± 1.9
ASF	18.0 ± 1.1	32.1 ± 3.8	-8.2 ± 1.9	-14.2 ±2.1

Table 7 : image quality from corner reflector analysis

Figures

Figure 1 : Data processed prior to 1996 by NASDA had a processing artifact (banding in range) in most images. The arrows indicate the locations of the bands in this example enhanced image from South America.

Figure 2 Approximate South and Central America coverage: a) GRFM coverage during September 27 - December 12, 1995. b) GRFM coverage during May 4- August 14, 1996.

Figure 3 Approximate Africa coverage: a) GRFM coverage during January - March, 1996. b) GRFM coverage during October-November, 1996. Also imaged was the island of Madagascar in early 1997.

Figure 4 : Approximate South East Asia and Australia coverage: GRFM coverage during November 1996 - February 1996.

Figure 5 : Histogram of a rainforest scene (center Latitude,Longitude : 02°,-60°). a) NASDA processed image (October 1993) - histogram of values for a typical rainforest image. The peak is at a DN of 979, or -8.68 dB b) ASF processed image (October 1995) - histogram of values of typical rainforest image. The peak is at a DN of 119, or -7.03 dB.

Figure 6 : During processing at both ASF and NASDA, a standard correction is applied to account for the change in antenna gain with look angle. During ASF processing, the inverse of this gain factor is saved as the "noise vector" in the CEOS leader file. This figure shows a typical example.

Figure 7 : polynomial fitted to the inverse of radiometric trend.

Figure 8 : a typical residual radiometric trend

Figure 9 : typical plot of the noise equivalent σ^0 , estimated by analysing the radar backscatter over open water (generally the darkest locations in the imagery) at several cross-track (range) locations. These areas are generally dominated by noise, rather than signal from the waves on the water.

Figure 10 : The histogram of offsets in the x (a) and y (b) direction applied to each scene while mosaicking 1500 scenes from South America.

Figure 11 : An image of the Balbinas Reservoir in Amazonas (from images averaged to 100 meter pixel spacing), Brazil, several hundred kilometers North of the city of Manaus. This image is 21 km x 18 km.

Figure 12 : An example of mosaicking two cross-track scenes covering the area where the Tapajos and Amazon Rivers converge. This image is 24 km x 23 km.

Figure 13: An image mosaic of two images where residual calibration errors are evident. This image is 10 km x 10 km.

Figure 14. A "slice" through values where calibration error exists in overlap region between two scenes.

Short Title : Data Quality of the JERS-1 SAR GRFM project

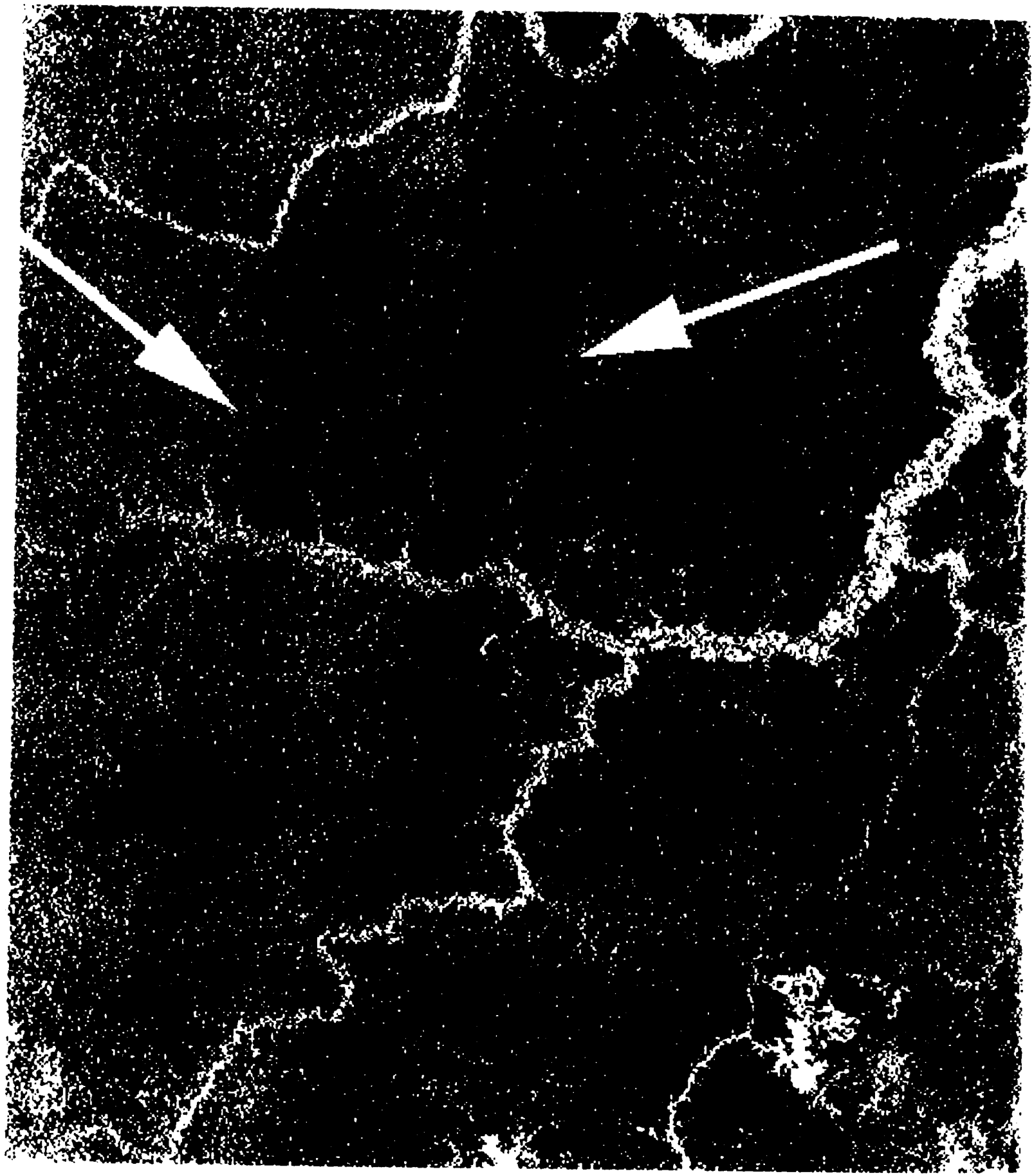

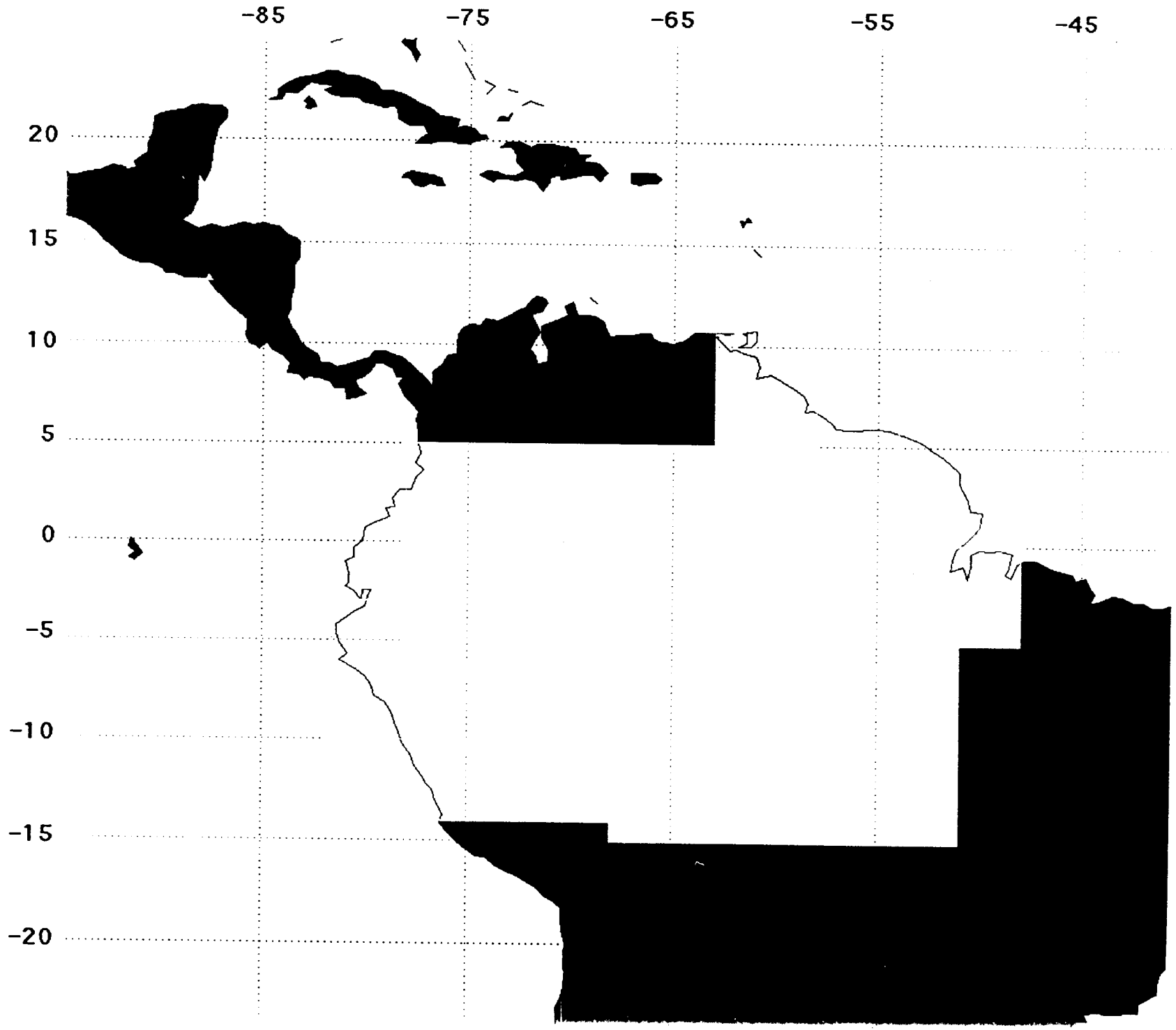
-85
-75
-65
-55
-45
20
15
10
5
0
-5
-10
-15
-20

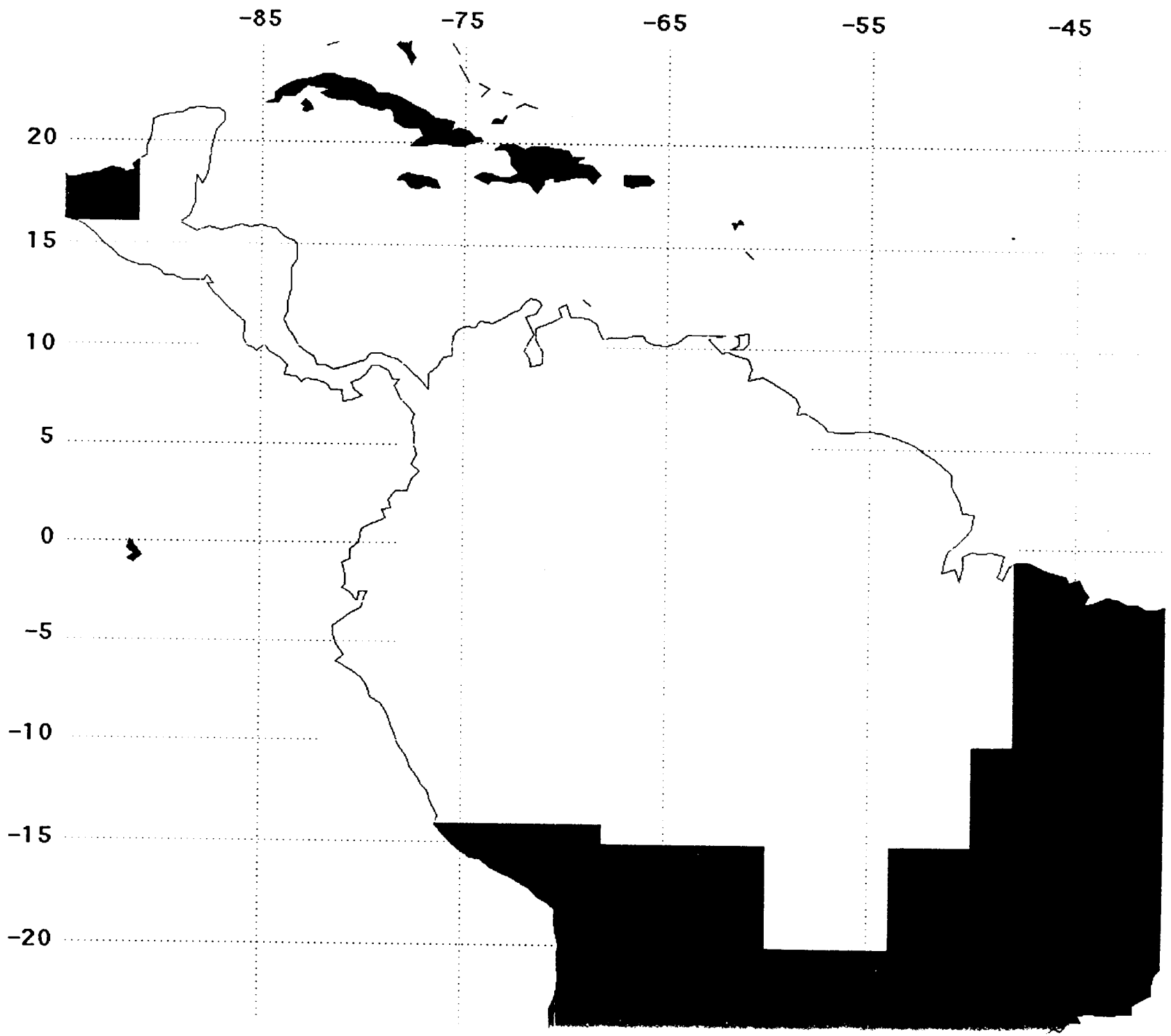
-85
-75
-65
-55
-45
20
15
10
5
0
-5
-10
-15
-20

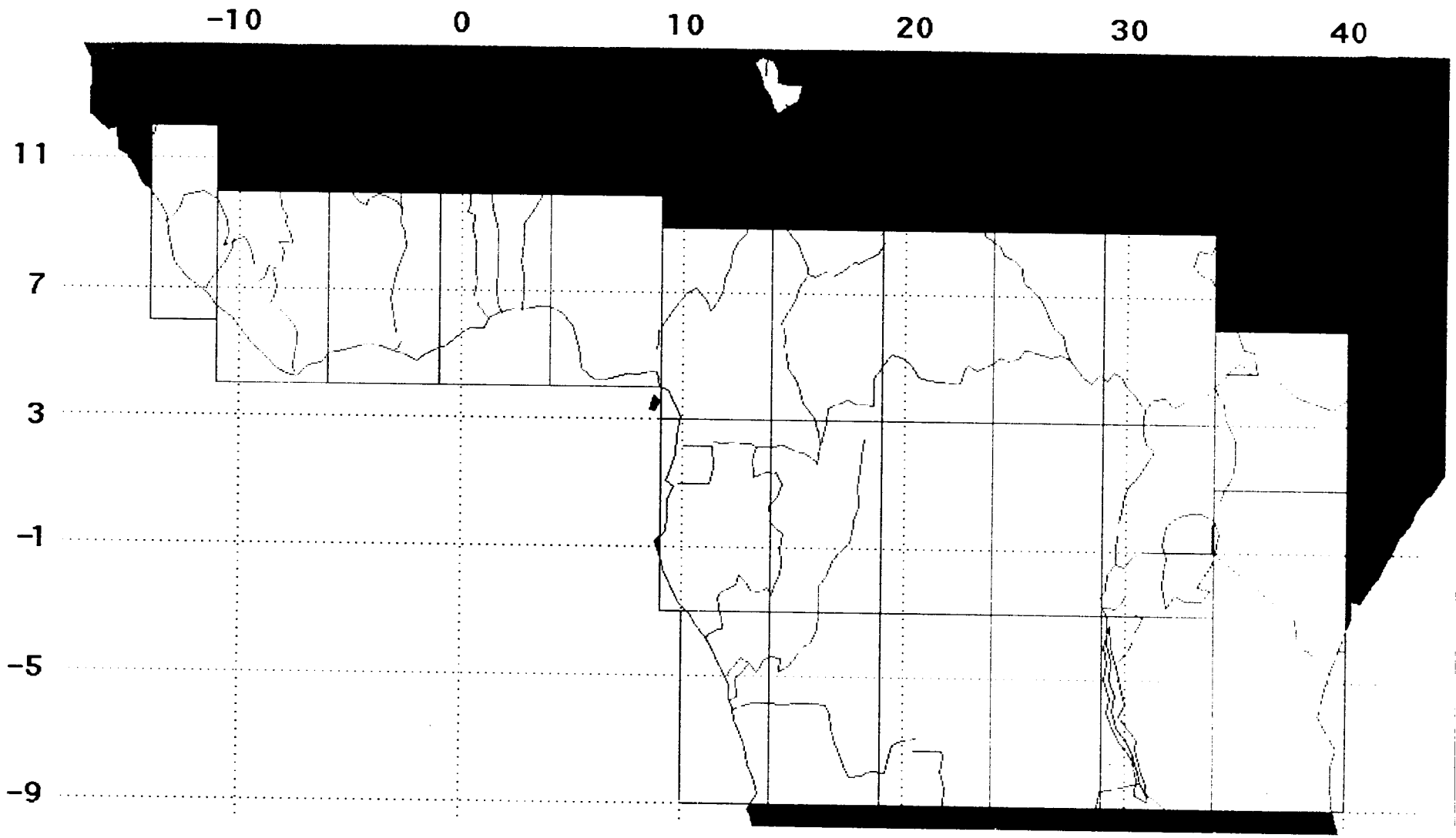
-10
0
10
20
30
40
11
7
3
-1
-5
-9

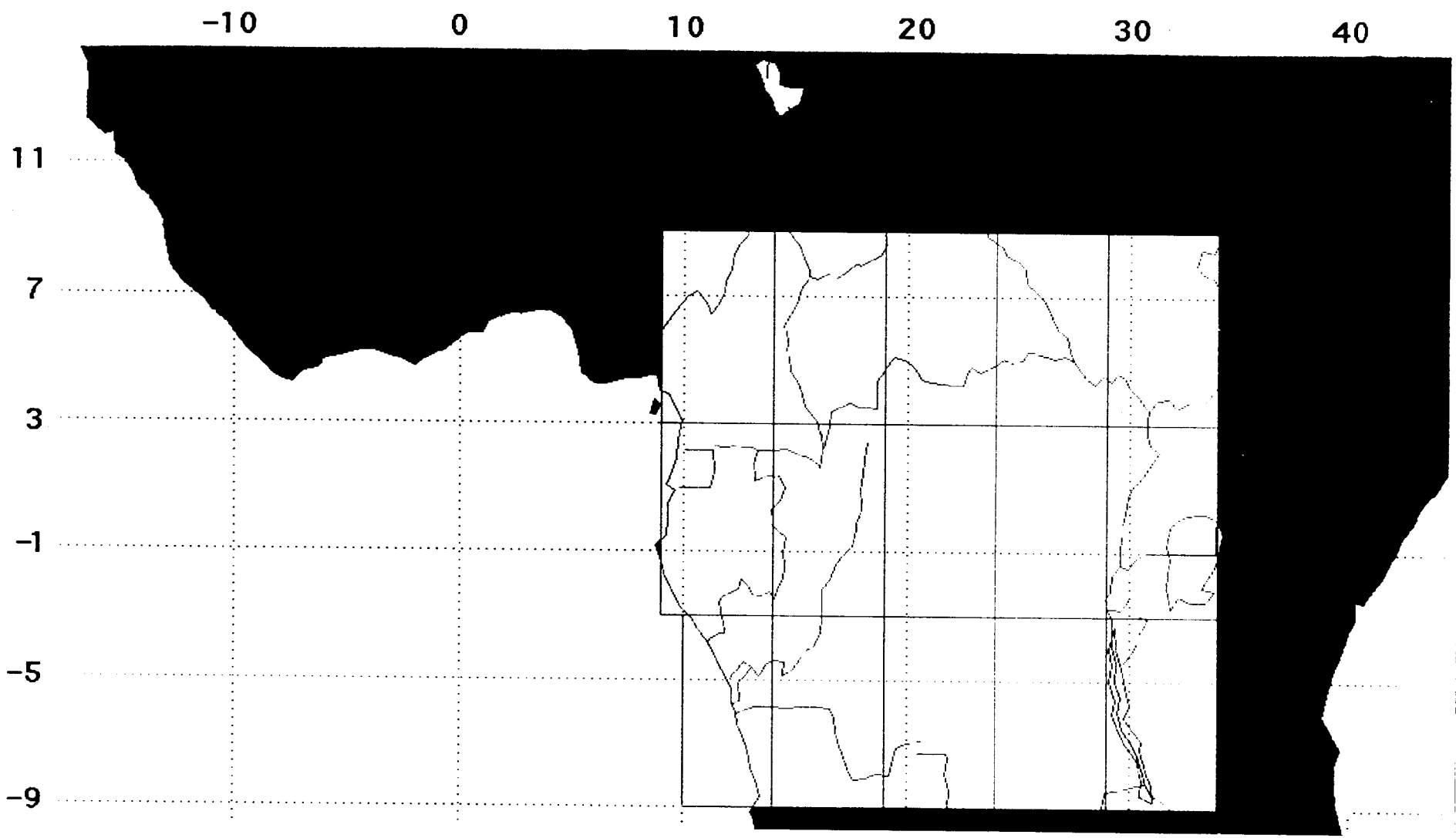
-10
0
10
20
30
40
11
7
3
-1
-5
-9

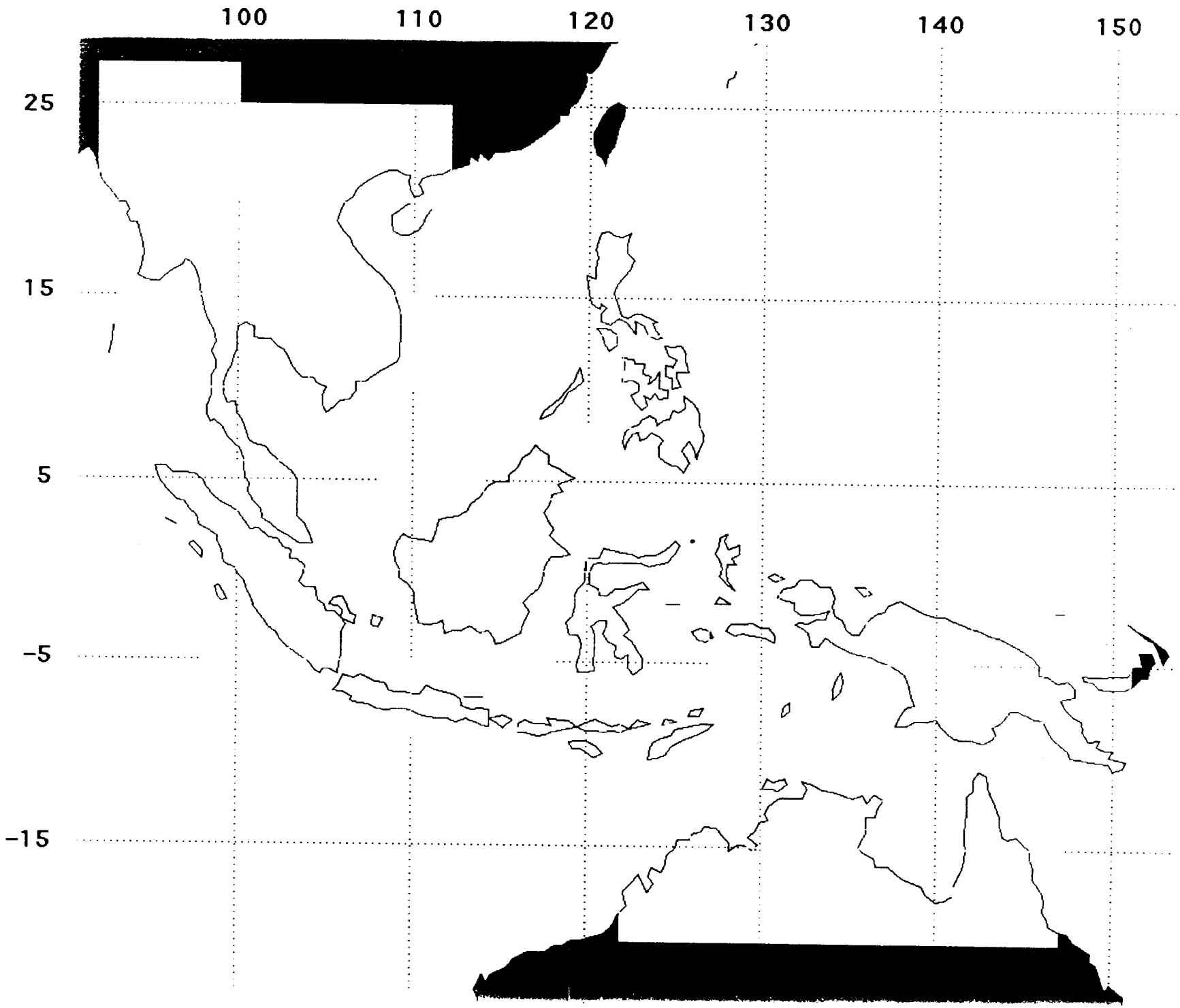
100
110
120
130
140
150
25
15
5
-5
-15

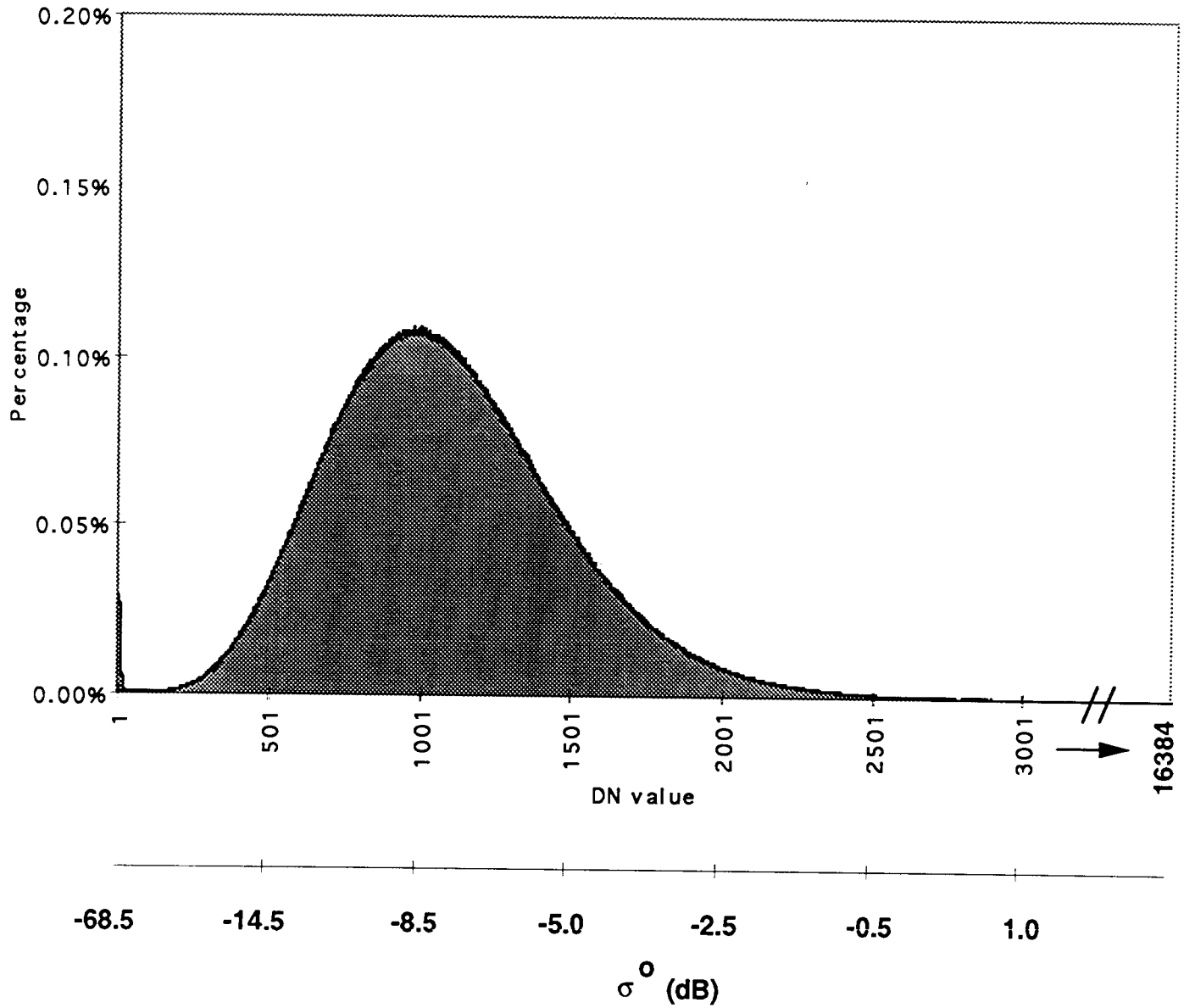
0.20%
0.15%
0.10%
0.05%
0.00%
Percentage
1
501
1001
1501
2001
2501
3001
16384
DN value
-68.5
-14.5
-8.5
-5.0
-2.5
-0.5
1.0
σ° (dB)

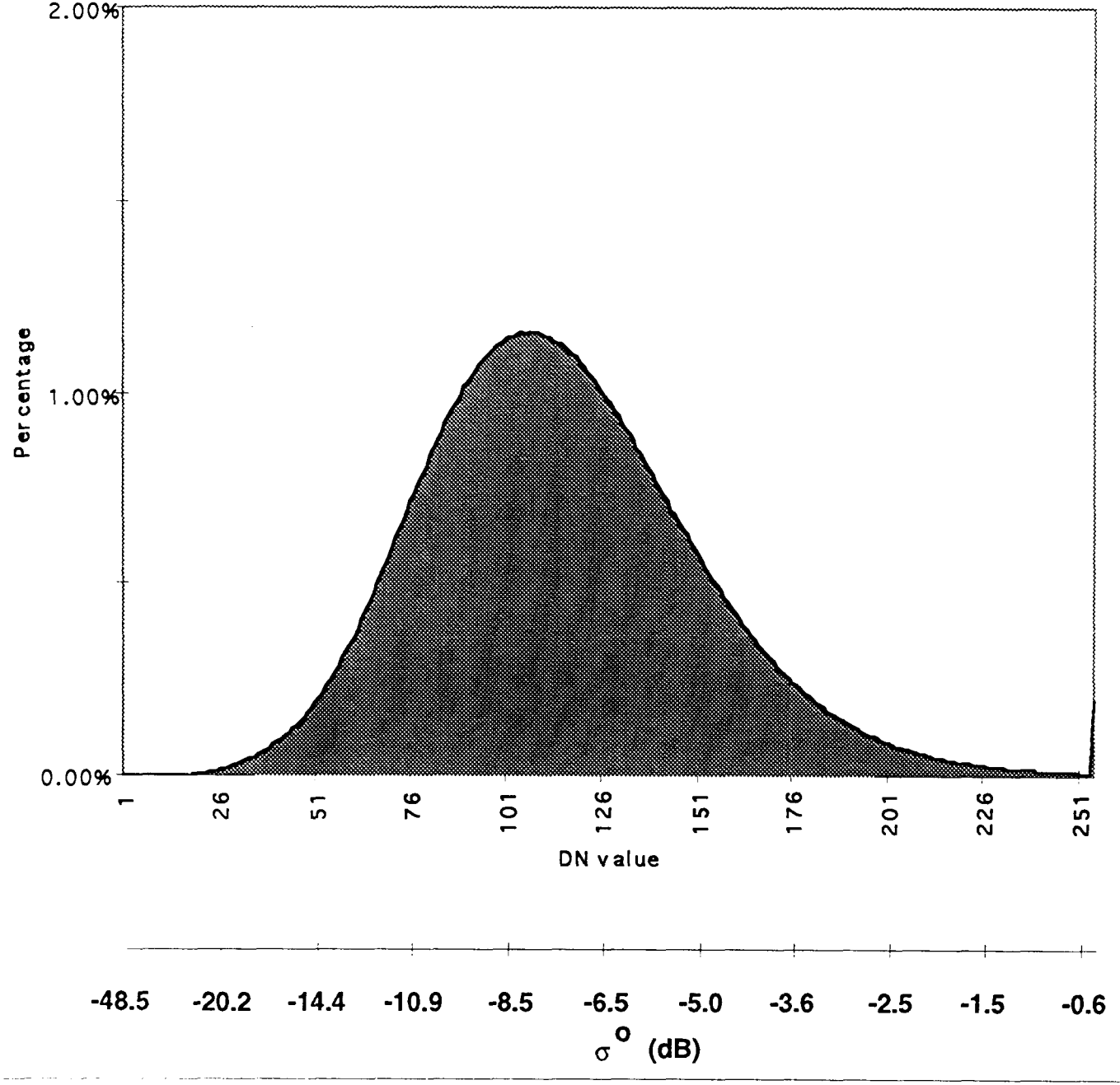
2.00%
1.00%
0.00%
Percentage
1
26
51
76
101
126
151
176
201
226
251
DN value
-48.5
-20.2
-14.4
-10.9
-8.5
-6.5
-5.0
-3.6
-2.5
-1.5
-0.6
σ° (dB)

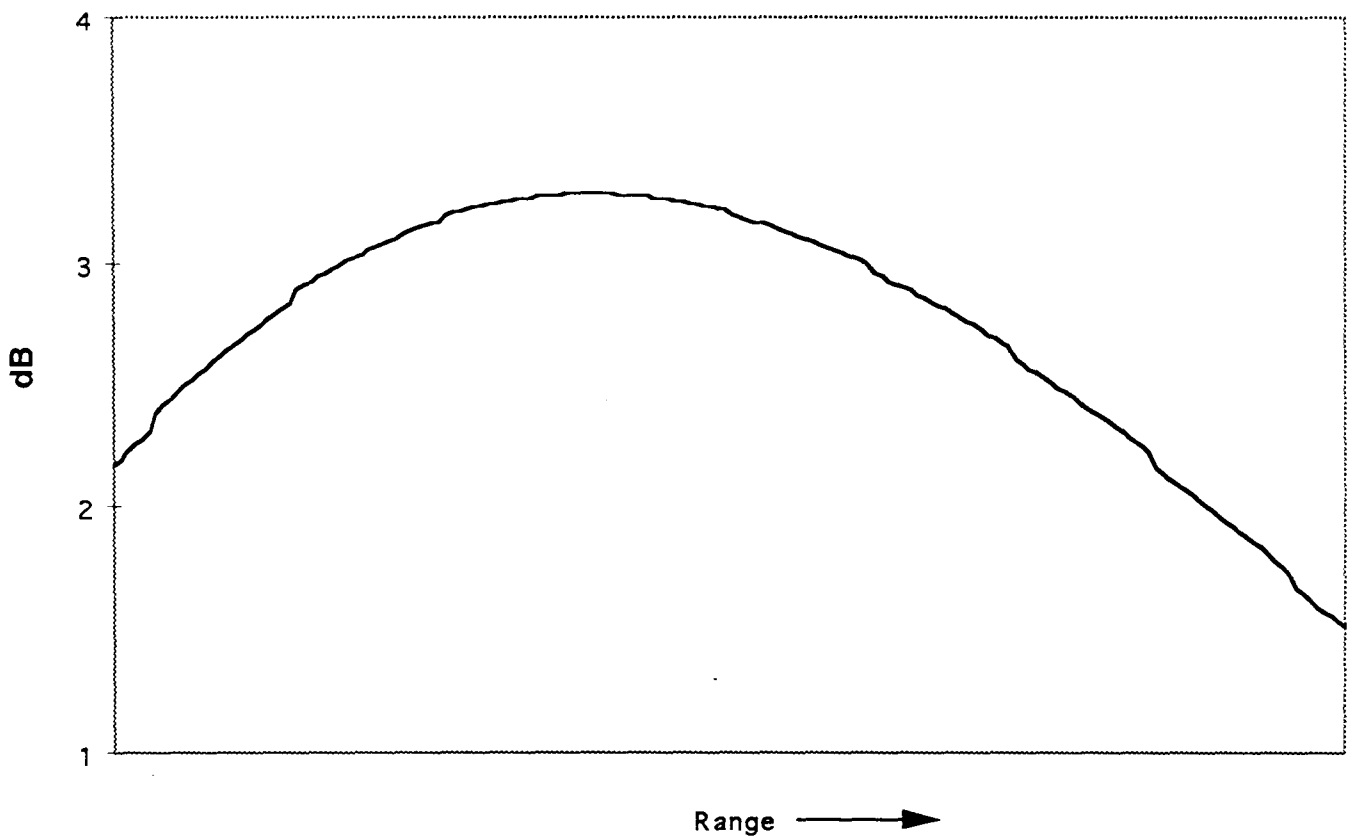
4
3
2
1
dB
Range

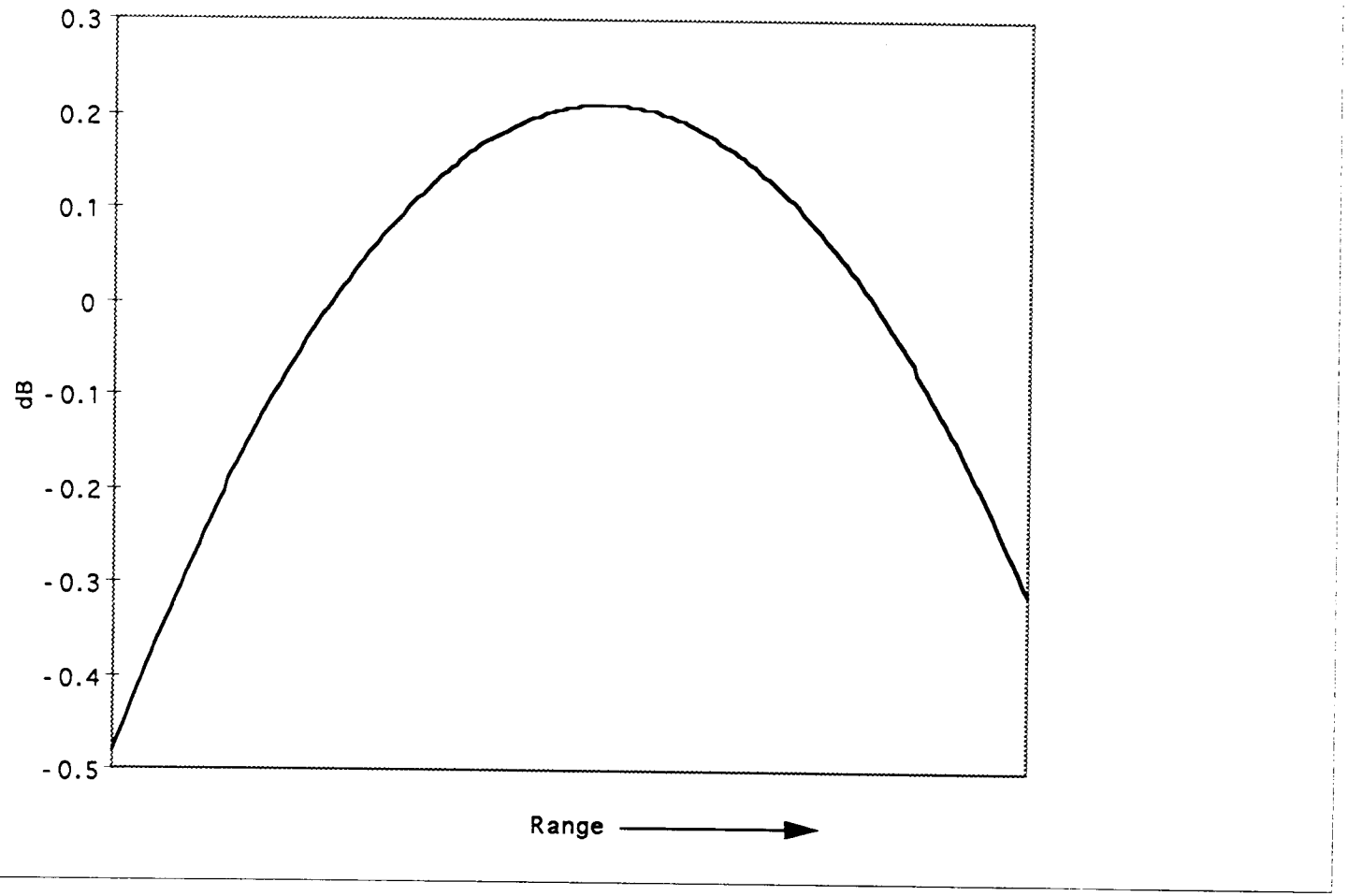
0.3
0.2
0.1
0
- 0.1
- 0.2
- 0.3
- 0.4
- 0.5
dB
Range

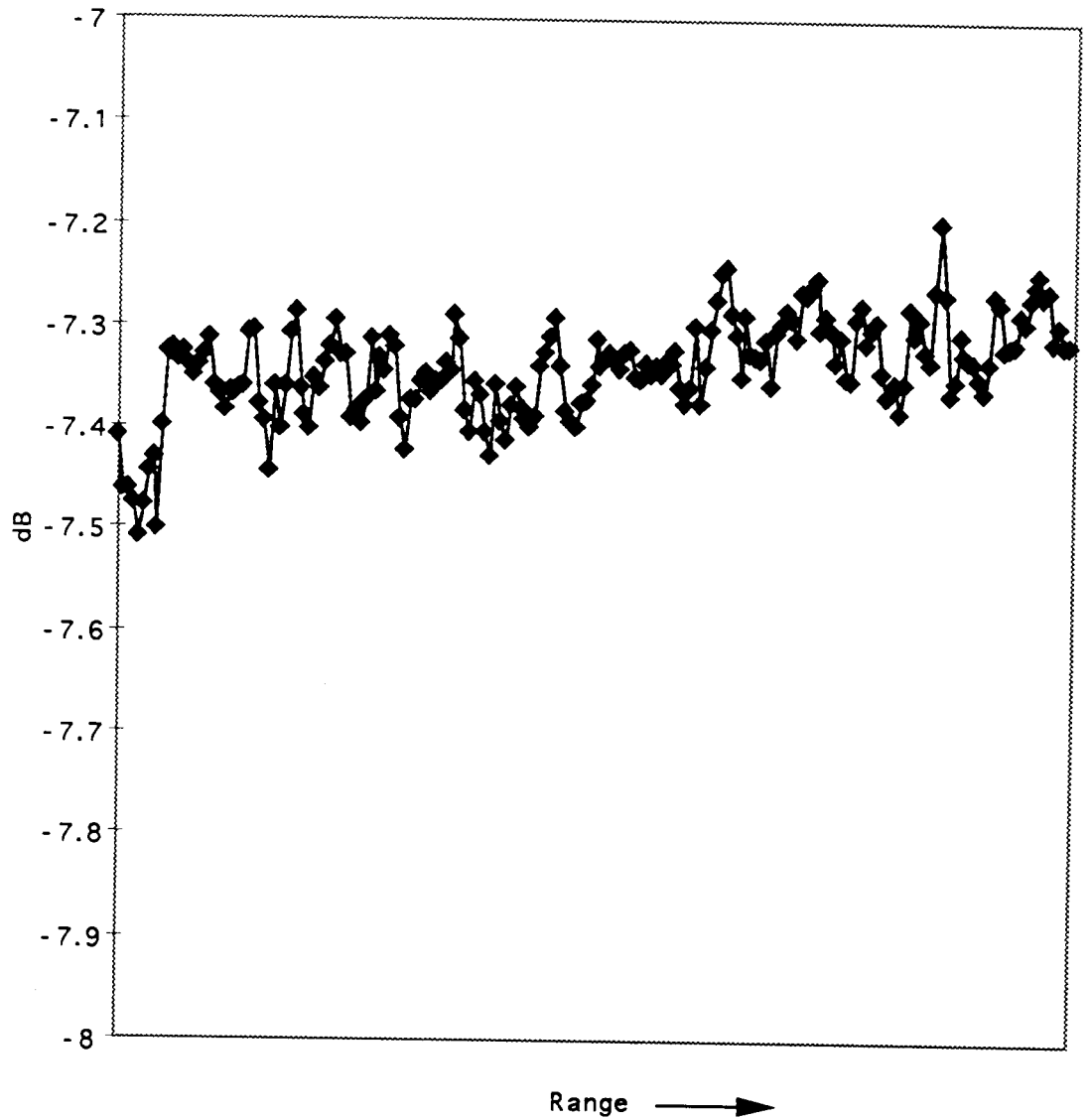
-7
-7.1
-7.2
-7.3
-7.4
-7.5
-7.6
-7.7
-7.8
-7.9
-8
dB
Range

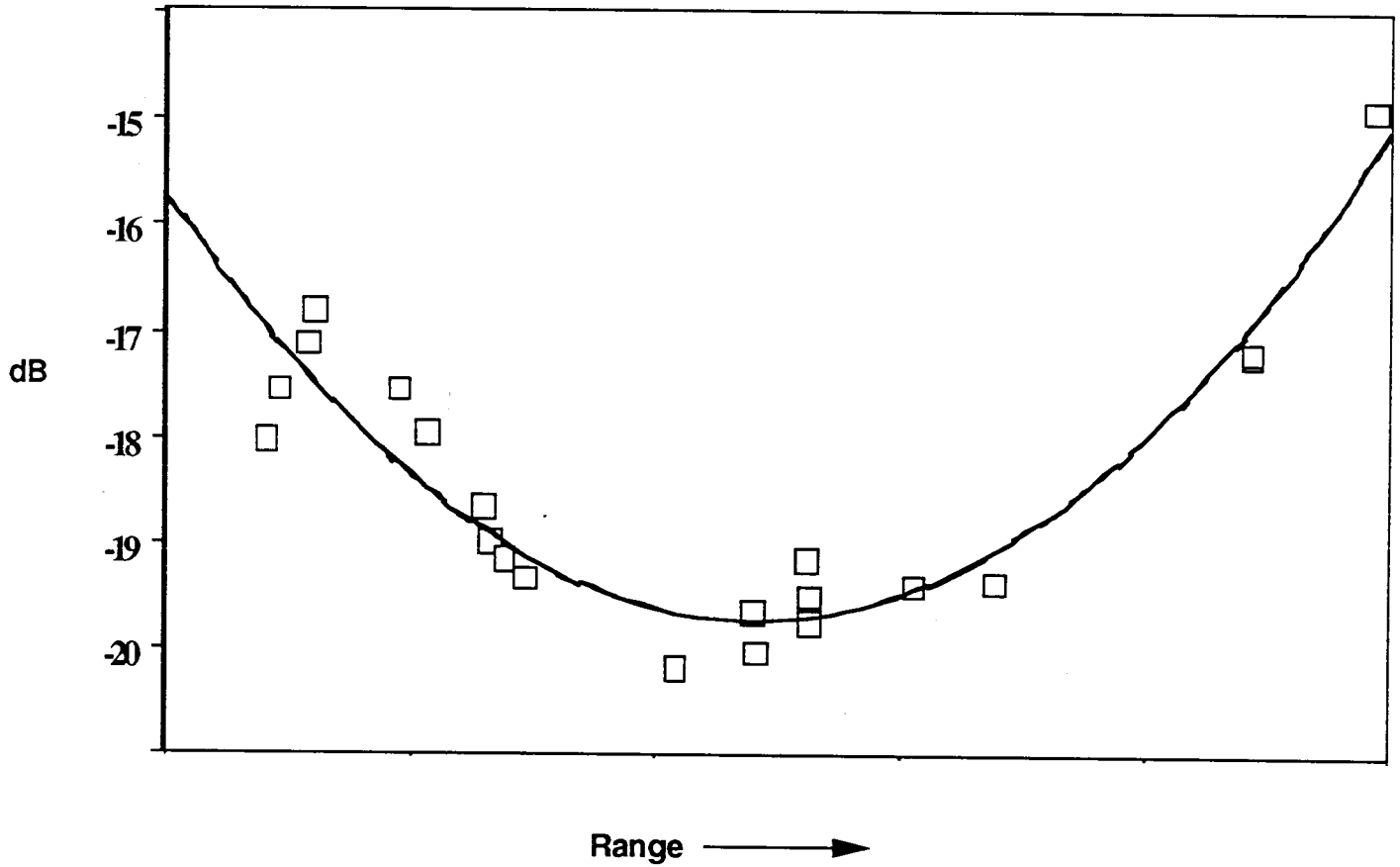
-15
-16
-17
-18
-19
-20
dB
Range

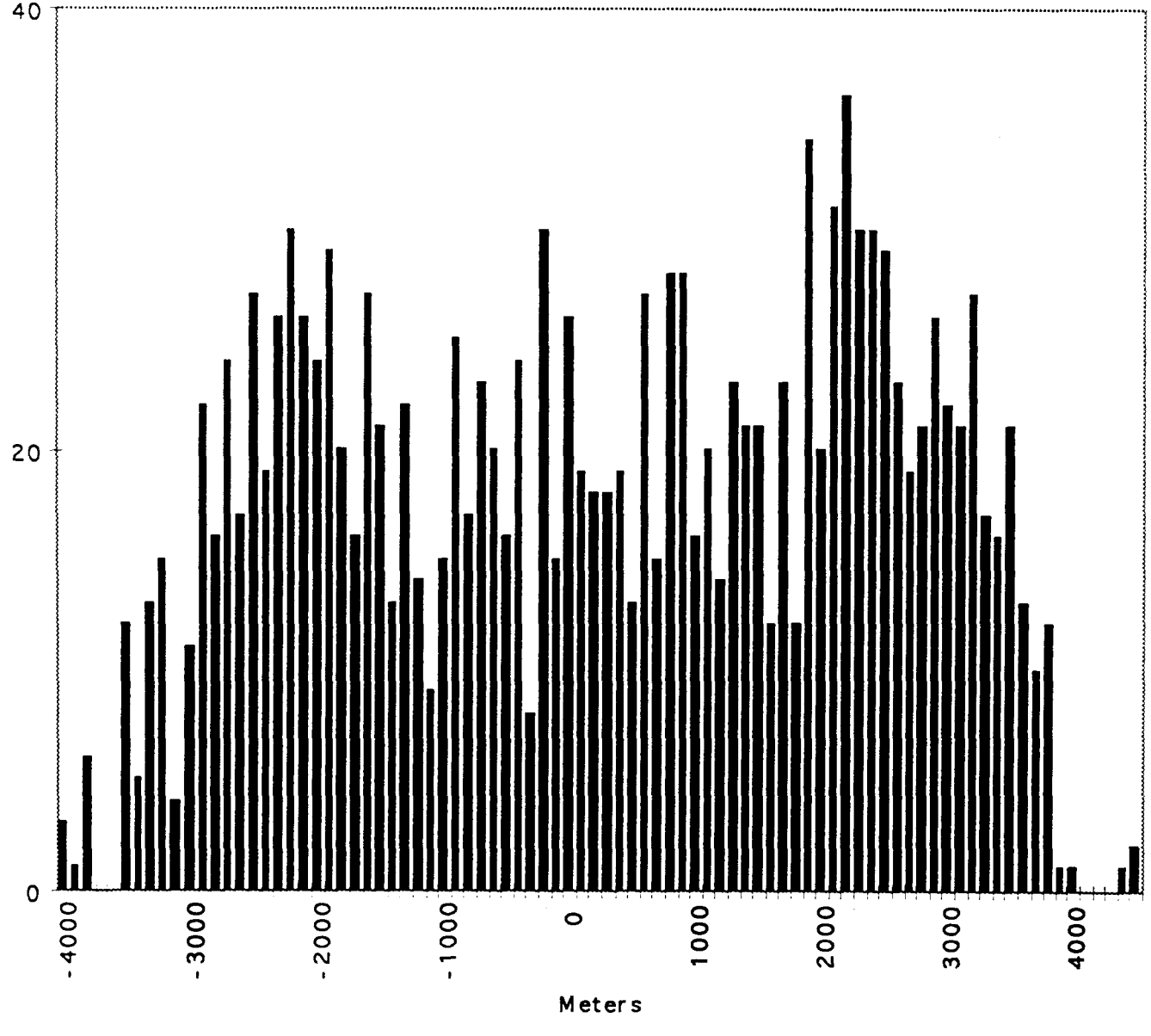
40
20
0
-4000
-3000
-2000
-1000
0
1000
2000
3000
4000
Meters

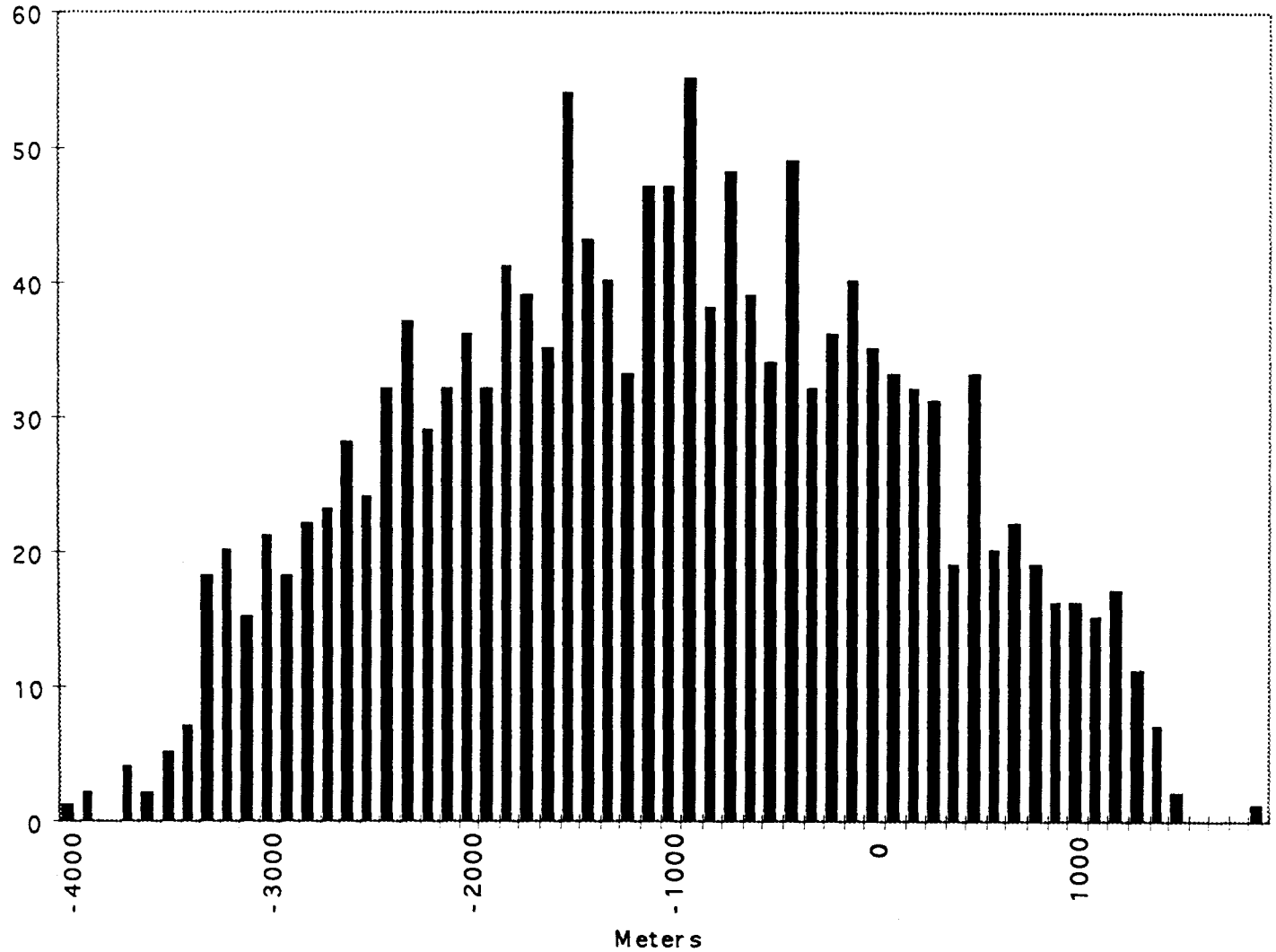
60
50
40
30
20
10
0
-4000
-3000
-2000
-1000
0
1000
Meters

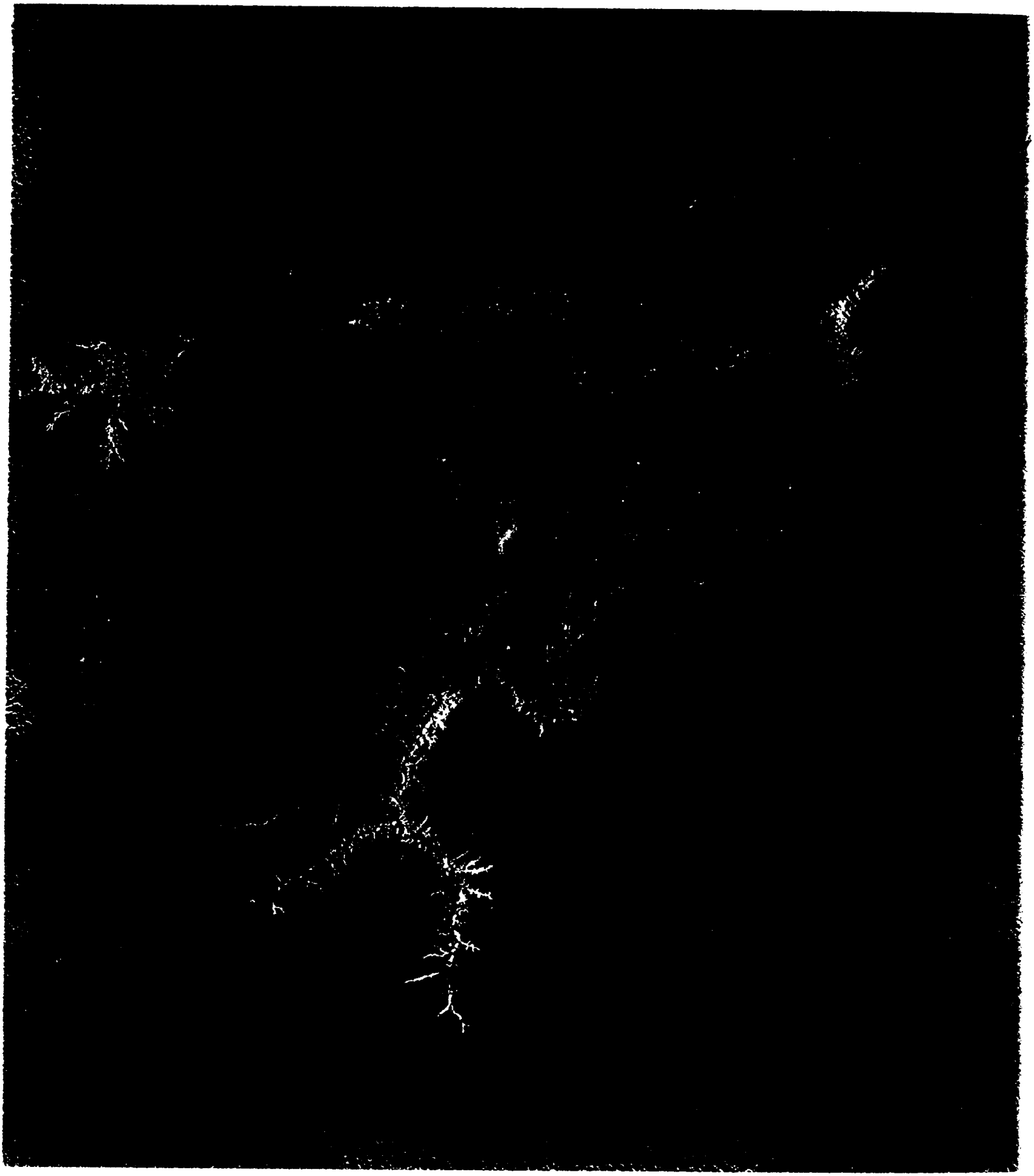

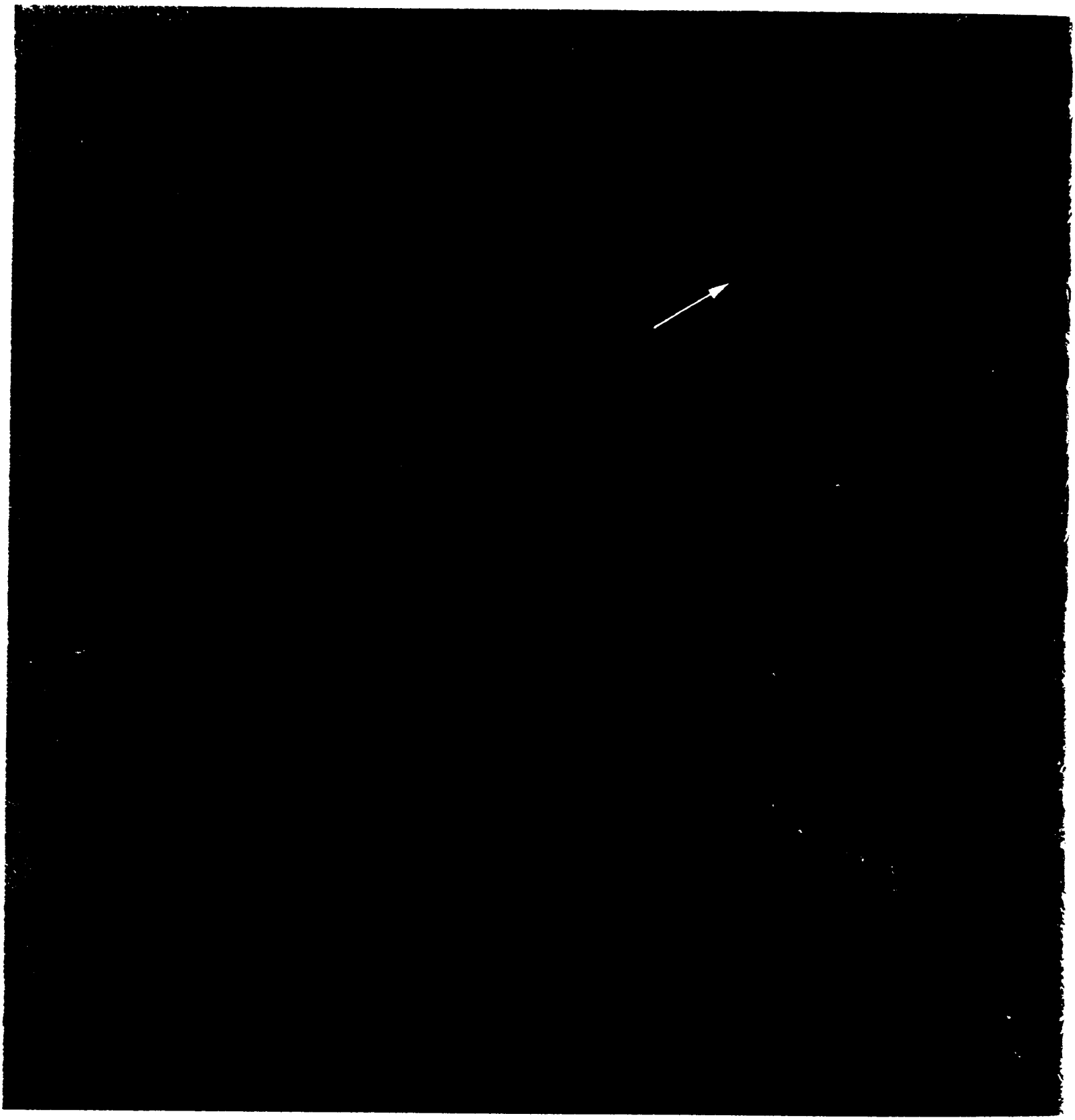

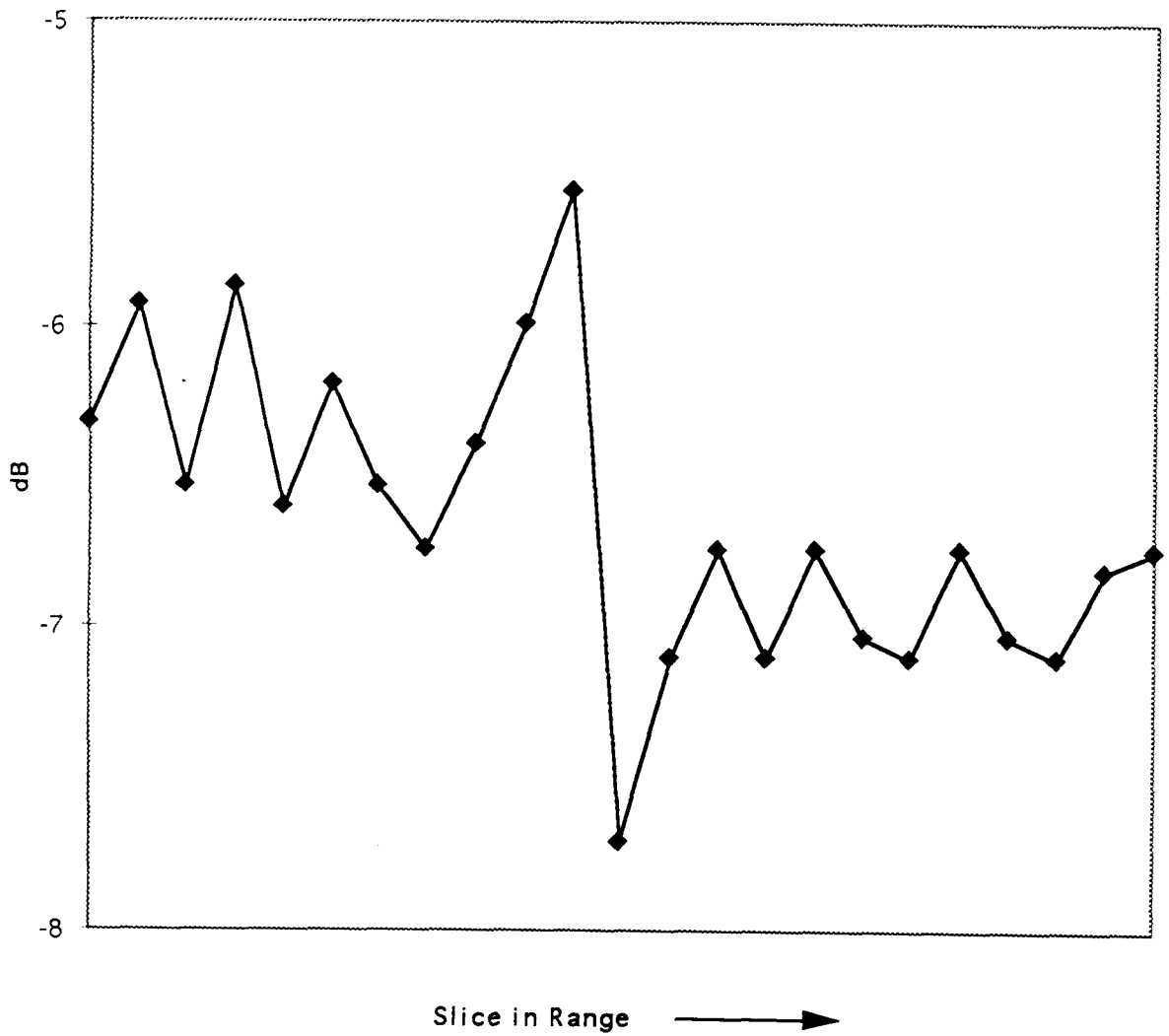
-5
-6
-7
-8
dB
Slice in Range